Journal of GeoEngineering, Vol. 11, No. 3, pp. 109-122, December 2016
http://dx.doi.org/10.6310/jog.2016.11(3).1

A SIMPLIFIED MODELING FOR SEISMIC RESPONSES OF RECTANGULAR FOUNDATION ON PILES SUBJECTED TO HORIZONTAL EARTHQUAKES

Der-Wen Chang [1*], Min-Ru Lee [2], Ming-Yang Hong [2], and Yen-Chih Wang [3]

ABSTRACT

This paper presents a simplified modeling for seismic responses of rectangular foundation on piles subjected to horizontal earthquakes. The motions of foundation can be derived simply assuming that the foundation is vibrating in one direction. Time-dependent foundation responses under the earthquake with a bevel angle to the foundation were able to decompose and compute in both longitudinal and transverse directions. Using the explicit finite difference scheme, discrete wave equation analysis was suggested presuming that the lateral boundaries of foundation are free of tractions. The pile-soil-pile and soil elements underneath the rectangular foundation were modeled by springs. Seismic motions of the equivalent piers representing for the pile-soil-pile elements were analyzed using one-dimensional analysis of the single piles. Seismic forces transmitting through these elements to the foundation were able to obtain. The superstructure influences can be monitored assuming that the ratio of superstructure displacement and foundation displacement is constant. The proposed solutions were found compatible to three dimensional finite element ones. Factors to influence the seismic responses of foundation are discussed. The proposed analysis is concluded to provide efficient solutions to the preliminary design of piled raft foundation.

Key words: Rectangular foundation, piles, seismic responses, analysis, horizontal earthquake.

1. INTRODUCTION

The piled raft foundation has been extensively used for massive and/or high-rise buildings located in soft ground sites and/or sites vulnerable to seismic liquefaction. The purpose of such foundation is to reduce the amount of settlements and differential settlements, and further to increase the lateral and overturning resistances of designed structures. The methods used in the design and analysis of such foundation have been suggested by Poulos (1991, 2001), Clancy and Randolph (1993), Randoplh and Clancy (1993), Katzenbach (1993), Randolph (1994), Yamashita *et al.* (1994), Horikoshi and Randolph (1996), Kobayashi *et al.* (2009), and Yamashita *et al.* (2015). According to Poulos (2001), they can be divided into three categories, 1. Simplified calculation methods (*e.g.,* the analytic formulas suggested by Poulos-Davis-Randolph), 2. Approximate computer-based methods (*e.g.,* a rectangular slab on springs, plate on springs, or the Hybrid method based on two-dimensional (2D) elements of plate with one-dimensional (1D) pile elements and soil springs), and 3. Rigorous computer-based methods (*e.g.,* Boundary Element Method (BEM), Finite Element Method (FEM), or Hybrid method combines both BEM and FEM). All these methods can provide rational solutions to different levels of design requirements.

At modern time, although three dimensional (3D) FEM analysis has been recognized as the most rigorous and powerful solution for piled raft foundation problems (Abderlrazaq *et al.* 2011; Katzenbach and Choudhury 2013; Katzenbach *et al.* 2013; Kouroussis *et al.* 2013), it is important to learn that the approximate type solutions can sometimes provide effective solutions as well. The computation time of such type solution would be much less than the 3D FEM analysis. Therefore the approximate computer-based method could provide a useful tool to the performance based design (PBD), in which a large amount of computations can be carried out on variability of design parameters. According to Kitiyodom and Matsumoto (2002, 2003), Kitiyodom *et al.* (2005), and Matsumoto (2013), 3D approximate computer-based methods have been suggested for static and dynamic analyses of piled raft foundation. These analyses were conducted solving the equations of motion established at the nodes of the discrete raft. The piles and the surrounding soils connecting to the slab were taken as the structural elements which can be treated as springs and dashpots. Figure 1 depicts the discrete layouts used in their static and dynamic analyses. These analyses are limited to the piled raft foundation where the loads are acting on top of the foundation. For seismic responses of the foundation caused by ground excitations, further studies need to be made.

In this paper, a simplified modeling on the seismic responses of piled raft foundation is presented. In monitoring seismic motion of the foundation, only the horizontal ground excitations were assumed. The approximate analysis is suggested solving the differential equation based on force equilibriums of the raft with central difference formulas. The causative seismic motions were able to find by Chang *et al.* (2014) solving the ground responses

Manuscript received February 15, 2016; revised May 26, 2016; accepted July 13, 2016.
[1] Professor (corresponding author), Department of Civil Engineering, Tamkang University, Tamsui District, New Taipei City, Taiwan (e-mail: dwchang@mail.tku.edu.tw).
[2] Graduate Student, Department of Civil Engineering, Tamkang University, Tamsui District, New Taipei City, Taiwan.
[3] Research Associate, Department of Civil Engineering, Tamkang University, Tamsui District, New Taipei City, Taiwan.

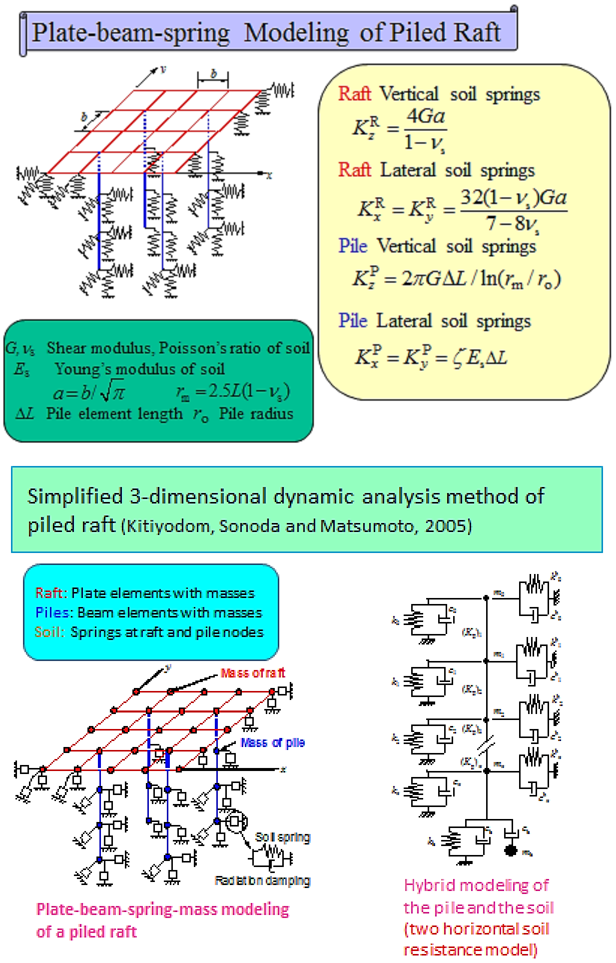

Fig. 1 **Schematic layout of approximate computer based methods (static and dynamic) for piled raft foundation (from Matsumoto, 2013)**

of a free-field and the corresponding ones for the installed piles. These motions can be used to find time-dependent displacements of the pile-soil-pile elements (or the equivalent piers) underneath the raft. The ground motions are thus applied to the raft with shear springs for the pile-soil-pile elements. With proper controls of the loads from superstructure and underlain soils, corresponding responses of the raft can be found. Figure 2 illustrates the computational procedures taken in proposed modeling. To validate the proposed analysis, 3D FEM analysis was conducted on a numerical model of a mega rectangular slab underlain by numerous piles. It can be found that using such approximate computer-based analysis, not only the influence of ground motion in oblique with the foundation can be analyzed, but also those effects associated with the design parameters (*i.e.*, pile diameter, pile length, number of piles, and the shear wave velocity of the soil) can be learnt easily.

2. GOVERNING EQUATIONS AND DISCRETE SOLUTIONS

Figure 3(a) shows the schematic layout of the uncoupled motions of a slab (*i.e.*, the spread raft of the piled raft foundation). The displacements in x, y and z directions are denoted as u, v and

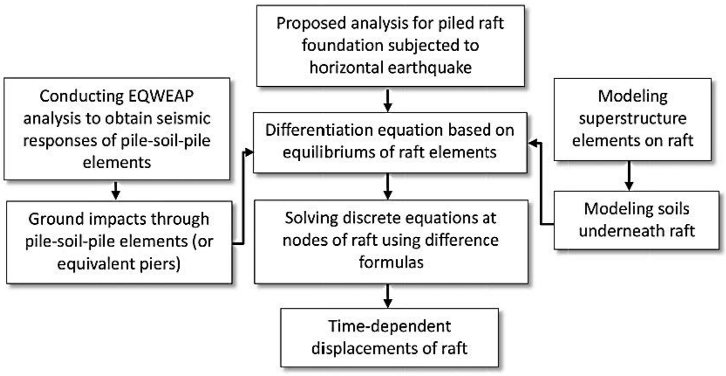

Fig. 2 **Computation procedures in the proposed modeling**

w, and the rotations along these axes are assumed relatively small and thus negligible. For horizontal earthquake shaking in the x direction, the governing differential equation for the motion of the slab can be derived based on force equilibriums of the raft (see Fig. 3(b)) as follows,

$$EA\frac{\partial^2 u}{\partial x^2}dx = \rho A dx \frac{\partial^2 u}{\partial t^2} + k_{sb}(u - u_g) + k_{ep}(u - u_{ep}) + k_{st}(1-R)\,u + m_{st}\,R\frac{\partial^2 u}{\partial t^2} \quad (1)$$

where u = displacement of the raft; u_g = displacement of the ground soil underneath the raft; u_{ep} = displacement of the equivalent pier (pile-soil-pile system) underneath the raft; E = Young's modulus of raft; A = cross-section area of the raft; ρ = mass density of the raft; k_{sb} = spring constant of the soils underneath the raft (units in Force/Length); k_{ep} = spring constant of pile-soil-pile system underneath the raft (units in Force/Length) which can be calculated as $k_p n + k_s A_s$, where k_p = stiffness of single pile; k_s = stiffness of the soils in equivalent pier; n = number of piles, A_s = area of the soils in equivalent pier; k_{st} = stiffness of the superstructure (units in Force/Length); R = ratio of the superstructure displacement divided by the raft displacement (*i.e.*, $R = u_{st}/u$), m_{st} = mass of the superstructure. Notice that the ratios are assumed the same for the displacements and the accelerations.

In some cases, k_{sb} can be found in Table 1 as suggested by Gazetas (1991). When using the discrete form of Eq. (1), one needs to be cautious about the length and width of the slab following the suggestions of Gazetas (1991). In this study, k_{sb} is simply treated as shear spring constant, *i.e.*, $G_s A_{sb}/l_s$, where G_s = shear modulus of the soil; A_{sb} = contact area of the soils outsides the pile-soil-pile elements; l_s = thickness of the soil. The stiffness parameters k_{ep} and k_{st} can be computed from shear springs too. In that case, $k_p = G_p A_p / l_p$ where G_p, A_p, and l_p are the shear modulus, cross-section area, and the length of the pile, respectively; $k_s = G_s / l_s$, $k_{st} = G_c A_c / l_c + G_m A_m / l_m$ where the subscripts c and m respectively denote for concrete structure and material inside the concrete structure. Notice that in Eq. (1), the viscous forces resulted from the superstructure and the soils underneath the raft are ignored. Using the central difference formulas, the above equation can be expressed as follows,

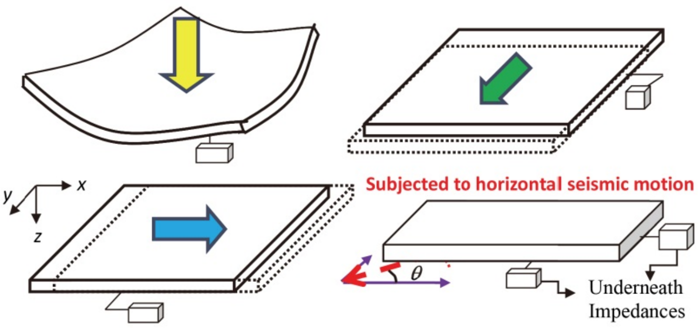

(a) Uncoupled motions of the slab

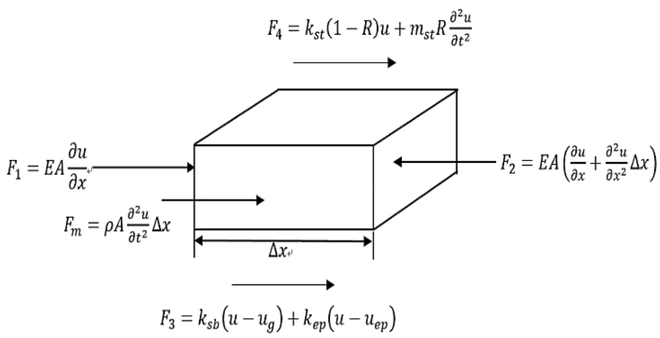

(b) Force equilibrium of foundation segment under horizontal excitations

Fig. 3 Uncoupled motions of raft foundation and force equilibrium on horizontal vibrations: (a) uncoupled motions and horizontal impact with a bevel angle to the foundation, (b) force equilibrium diagram

Table 1 Soil spring constants underneath the foundation (after Gazetas, 1991)

Vibration mode	Dynamic Stiffness $\mathbf{K} = K \times \kappa(\omega)$		
	General shape ($2L \times 2B$, $L > B$)	Square $L = B$	Dynamic Stiffness Coefficient $\kappa(\omega)$
Vertical	$Kz = \dfrac{2GL\times(0.73+1.54\chi^{0.75})}{(1-\nu)}$	$Kz = \dfrac{4.5GB}{(1-\nu)}$	$\kappa = f(L/B,\ \nu,\ a_0)$ $k_{avg} \cong 1.0$ for $L/B = 1 \sim 5$
Horizontal, y (in transverse direction)	$Ky = \dfrac{2GL\times(2+2.50\chi^{0.85})}{(2-\nu)}$	$Ky = \dfrac{9GB}{(2-\nu)}$	$\kappa = f(L/B,\ a_0)$ $k_{avg} \cong 1.2$ for $L/B = 1 \sim 5$
Horizontal, x (in longitudinal direction)	$Kx = Ky - \dfrac{0.2GL\times(1-B/L)}{(0.75-\nu)}$	$Kx = Ky$	$\kappa \cong 1.0$

Note: $\chi = A_b/4L^2$, A_b = contact area of the foundation, G = Shear Modulus of soil, ν = Poisson's ratio of soil, a_0 = dimensionless frequency (= $\omega r / Vs \cong 0 \sim 2$ where ω = circular frequency, r = equivalent radius of the foundation, Vs = shear wave velocity of the soil)

$$\frac{1}{(\Delta x^2)}[u(i+1,j)-2u(i,j)+u(i-1,j)]$$
$$=\left(\frac{\rho}{E(\Delta t^2)}+\frac{m_{st}R}{\Delta x EA(\Delta t^2)}\right)[u(i,j+1)-2u(i,j)+u(i,j-1)]$$
$$+\frac{k_{sb}}{\Delta x EA}\left(u(i,j)-u_g(i,j)\right)+\frac{k_{ep}}{\Delta x EA}\left(u(i,j)-u_{ep}(i,j)\right)$$
$$+\frac{k_{st}}{\Delta x EA}(1-R)u(i,j) \tag{2}$$

Rewriting Eq. (2), the displacement of raft can be solved using Eq. (3) as follows.

$$u(i,j+1)=\left[\frac{(2F-2-B-C+D-H)}{F}u(i,j)+\frac{1}{F}u(i+1,j)\right.$$
$$\left.+\frac{1}{F}u(i-1,j)-u(i,j-1)+\frac{C}{F}u_{ep}(i,j)+\frac{B}{F}u_g(i,j)\right] \tag{3}$$

where $F=\dfrac{\rho\Delta x^2}{E(\Delta t^2)}+\dfrac{m_{st}R\Delta x}{EA(\Delta t^2)}$; $B=\dfrac{k_{sb}\Delta x}{EA}$; $C=\dfrac{k_{ep}\Delta x}{EA}$; $D=\dfrac{k_{st}\Delta xR}{EA}$; $H=\dfrac{k_{st}\Delta x}{EA}$; Δx = spatial increment in x direction; Δt = time increment. Notice that the motion of raft is assumed only occurring in the same direction of the seismic motion, tilting of the raft which may cause displacements in the transverse direction of the foundation is neglected.

The discrete equation is expressed in the explicit form in which the raft displacement u at the $(j+1)^{th}$ time step for the i^{th} node can be computed as a function of the i^{th}, $(i-1)^{th}$, and $(i+1)^{th}$ nodal displacements at the j^{th} time step, and the i^{th} nodal displacement at the $(j-1)^{th}$ time step as well as the displacements of equivalent pier and soils underneath the raft that occurring for the i^{th} node of the raft at the j^{th} time step. Similarly, the differential equation for the motion (displacement of v) of the slab due horizontal ground motion in y direction can be presented in the same manner differentiating the variable v with respect to y. If vertical motions, w of the raft were interested, the 4^{th} order partial differential equation with respect to x, y, and t should be analyzed. In that case, matrix analysis will be conducted at each time increment to solve for the foundation displacements in x-y directions.

As to the lateral boundaries of the raft, free tractions were considered simply assuming it as a surface foundation. Normal stresses at the ends of the raft are assumed zero. Equations (4) and (5) can be achieved with the assumptions that no superstructure and underneath pile-soil-pile elements and soil elements are encountered at the boundaries. To solve for the raft displacements, initial displacements and velocities of the raft foundation were set to zero by assuming that foundation is initially at rest prior to the seismic load. Time dependent raft displacements are thus obtained in an explicit manner.

Left end:

$$u(i,j+1)=\left[\frac{(2P-2)}{P}u(i,j)+\frac{2}{P}u(i+1,j)-u(i,j-1)\right] \tag{4}$$

Right end:

$$u(i, j+1) = \left[\frac{(2P-2)}{P} u(i, j) + \frac{2}{P} u(i-1, j) - u(i, j-1) \right] \quad (5)$$

where $P = \dfrac{\rho \Delta x^2}{E(\Delta t^2)}$

For horizontal seismic ground acceleration, $a(t)$ acting to the foundation with a bevel angle of θ as shown in Fig. 3(a), the analysis needs to be conducted independently taking into account of the acceleration's components $a(t)\cos\theta$ and $a(t)\sin\theta$ in each direction. The absolute displacements of the raft in direction of the causative ground acceleration could be calculated as $(u^2+v^2)^{0.5}$; displacement time history of the foundation can be converted from the x- and y-directional displacements and averaging them to yield the solution. The above analysis proposed in this study is termed as EQPR (EarthQuake analysis for Piled Raft foundation).

2.1 Responses of Pile-Soil-Pile Elements

The time-dependent displacement functions of the pile-soil-pile elements underneath the raft due horizontal ground motions can be analyzed using the EQWEAP procedure (Chang *et al.* 2014). In the first step, the linear and/or nonlinear free-field ground responses are able to obtain using the lumped mass analysis assuming that the ground is composed by horizontal soil layers. Secondly, the ground responses are applied to the discrete wave equations of the pile elements in order to solve for the corresponding pile displacements. Figure 4 illustrates the schematic layout of the EQWEAP procedure and the equilibriums of the pile segments used in the analysis. Notice that both the soil and pile nonlinearities can be modeled using proper material laws.

This solution was suggested in the past years and it was found reliable in comparison with the FEM analysis and pseudo static solution in matching the field observations (Chang *et al.* 2014; Chang *et al.* 2016). Although the EQWEAP analysis is suggested for single piles, with proper calculations of the load distributions while the effects of pile-to-pile interactions were included (Chang *et al.* 2009), this analysis can be used to monitor any single pile response within a pile group. In general, the piles were found moving accordingly with the ground motions. The differences between them are able to neglect. In applying the EQWEAP analysis into the piled raft foundation problem, it is suggested to obtain the response of the pile-soil-pile elements (or the equivalent pier), u_{eq} in connection with the raft (see Fig. 5) as follows,

$$u_{eq} = (u_p \sum A_p + u_{fd} \sum A_s) / (\sum A_p + \sum A_s) \quad (6)$$

In the above equation, u_p = time-dependent displacement function of the single piles; u_{fd} = free-field response function of the surface ground soil; $\sum A_p$ is the total cross-section area of the piles and $\sum A_s$ is the total area of surface soils in the pile-soil-pile elements. This would help to calculate the seismic ground force in Eq. (3).

2.2 Responses of Superstructures

The loads from the superstructure acting on top of the piled raft can be simulated as a single degree of freedom system (SDOF) and/or multiple degrees of freedom system (MDOF) represented by a set of mass-spring-dashpot elements. In Eq. (3), the formulation is presented for the forces transmitting only through a spring-mass system. A displacement ratio R, defined as the ratio of superstructure displacement u_{st} divided by foundation displacement u, will make the computations much easier. The same quantity of R is also assumed for the ratios of accelerations. It is important to point out that R between 0 ~ 1.0 is assumed for relatively rigid superstructure, in which the response of superstructure would be smaller than or equal to the foundation. For relatively flexible superstructure, the value of R could exceed 1.0, which indicates that the superstructure's response could be larger than the foundation's. If R became negative values, the superstructure and the foundation will vibrate asynchronously. The analysts may change the values of R in a rational manner to see how the foundation is affected by the characteristics of the superstructure.

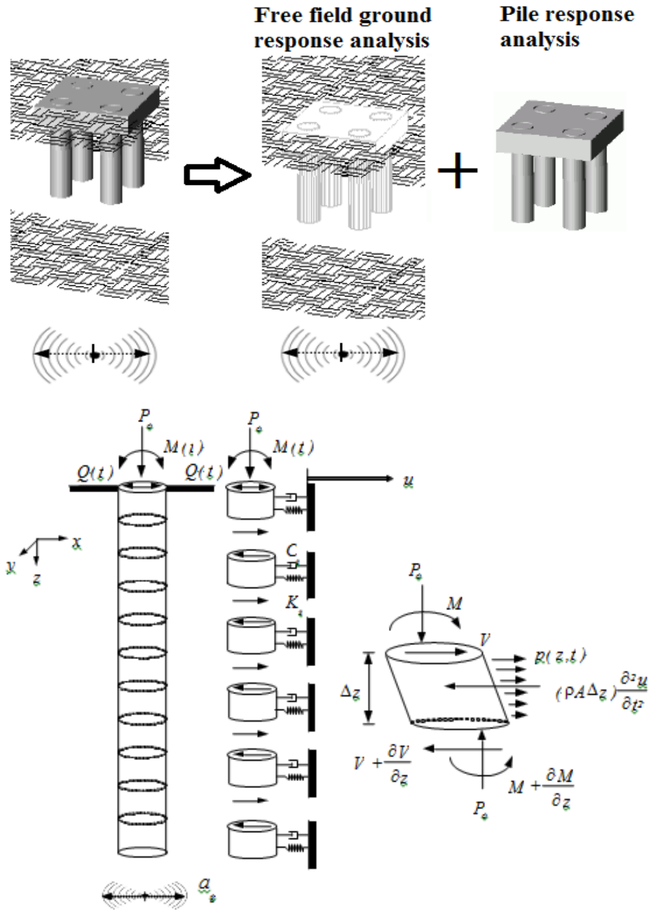

Fig. 4 Schematic layout of the EQWEAP analysis and equilibrium of pile elements

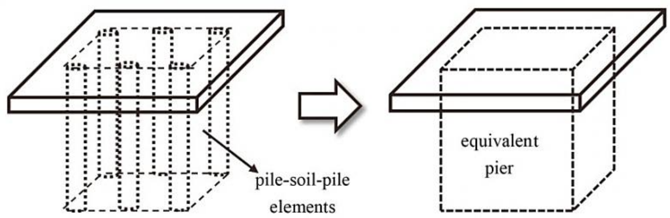

Fig. 5 Pile-soil-pile elements transformed to equivalent pier underneath the raft

3. NUMERICAL EXAMPLE AND VALIDATION

Assuming that a rectangular concrete slab with dimensions L × B × H = 300 m × 60 m × 2 m is allocated at the surface of a ground site consisting of soft soils whose thickness is 13 m and underlain by gravels. Five massive superstructures are evenly lined up on the slab. For each one of them, 81 concrete piles with pile diameter of 2 m and pile length of 28 m, oriented in a ring shape with radial distance at 7, 14, 21 and 26 meters from the central pile (see Fig. 6) are installed under the slab (where the size is 60 m × 60 m) to support the superstructures. In addition at each corner of the slab, three piles were seating in a triangular shape. As a result, each superstructure is supported by 93 concrete piles under the slab. Total number of the piles is 465. Material properties and model parameters used in the proposed analysis and the 3D FEM modeling using Midas-GTS program (Midas, 2012) are tabulated in Table 2. Seismic accelerations recorded at the TAP052 station in EW direction during the 1999 Chi-Chi earthquake is taken as the input of ground motion. Figure 7 shows the acceleration records obtained by a calibrated one based upon the designed Peak Ground Acceleration (PGA) at 0.24 g and the alternative one fitting acceleration record with the designed spectrum under the same level of PGA. It can be seen that although the time-dependent accelerations are in similar forms, the resulting response spectra are very different. One ought to be careful about the calibrations of artificial earthquake. Figs. 7(b) and 7(c) were obtained after baseline corrections.

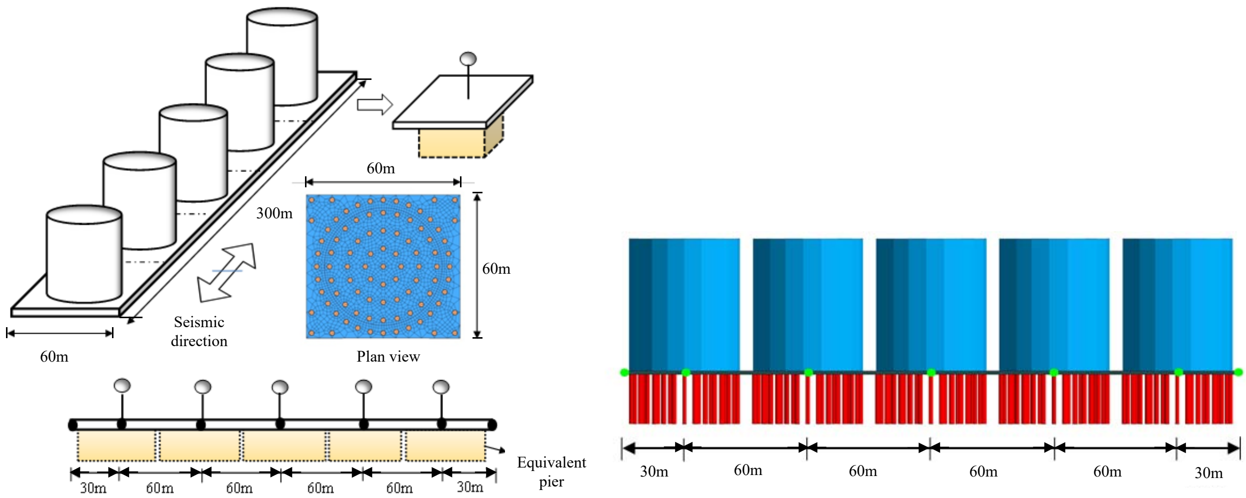

Fig. 6 Numerical model of rectangular foundation on piles and discrete nodes in the analysis

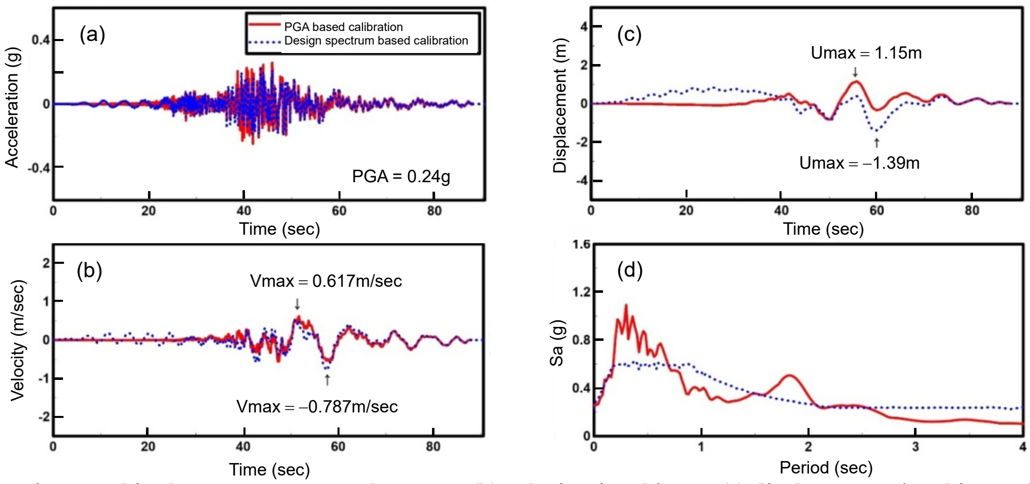

Fig. 7 Ground motions used in the analysis, (a) accelerogram (b) velocity time history (c) displacement time history (d) response spectrum of Sa

Table 2 Material properties and model parameters used in EQPR and 3D Midas-GTS analyses

<table>
<tr><th>Method</th><th>Material properties</th><th>Model parameters</th></tr>
<tr><td>EQPR analysis</td><td rowspan="2">Piles and raft: E = 3 × 10^4 MPa; γ = 24 kN/m^3; ξ = 0.02; ν = 0.1;
Soft soils: E = 137.4 MPa; Vs = 180 m/sec, γ = 14 kN/m^3; γ_{sat} = 16 kN/m^3; ξ = 0.05; ν = 0.3
Gravel: E = 1582.4 MPa; Vs = 560 m/sec; γ = 20 kN/m^3; γ_{sat} = 22 kN/m^3; ξ = 0.05; ν = 0.25</td><td>Pile, raft, soft soils and gravel: linearly elasticity</td></tr>
<tr><td>3D Midas-GTS analysis</td><td>Piles and raft : Linearly elasticity
Soft soils: Modified Cam Clay model
c = 19.6 kPa (0.2 kg/cm^2); ϕ = 35°; OCR = 1.0; λ = 0.087; κ = 0.0073;
e_0 = 1.042; M = 1.24; k_0 = 0.48
Gravel: Mohr Coulomb model
c = 0 kPa; ϕ = 36°; k_0 = 0.41</td></tr>
</table>

The analysis is then conducted with the input seismic motions using the first method. Horizontal seismic motion is assumed independently in the longitudinal and transverse directions of the foundation whereas the bevel angle is kept as 0° and 90°, respectively. For analysis in *x* direction, seven nodes along the raft are analyzed. For analysis in *y* direction, three nodes are computed. Notice that time increment used in the proposed analysis is 0.0005 sec to ensure stability of the solutions (the original data has time increment at 0.005 sec). The discrete model used in 3D FEM modeling is shown in Fig. 8. Convergence and stability of the FEM solutions were ensured varying the types of elements, discrete mesh, and boundary conditions.

Figure 9 depicts the results from the EQPR analysis and the solutions from 3D Midas-GTS analysis assuming that there is no superstructure on top of the foundation. It can be found that the solutions are rationally compatible providing that the stability of solutions is ensured. The time increment used in Midas analysis is 0.02 sec. It is interesting to learn that the ground motions acting in *x* direction (longitudinal direction of the slab) will yield very small difference (digits after the decimal point) than those acting in *y* direction (transverse direction of the slab). This observation will be discussed further when the superstructure loads were encountered. Figures 9(c) and 9(d) depicted the internal bending moments and shear forces at the time (55.8 sec) when the maximum displacements occurred. The FEM and simplified solutions have some disagreements since the nonlinearities of the structure were captured by different material models. Various stress conditions at the pile heads will also affect the results. More comparisons on the internal stresses of the piles from different numerical modeling can be found in Hong (2016).

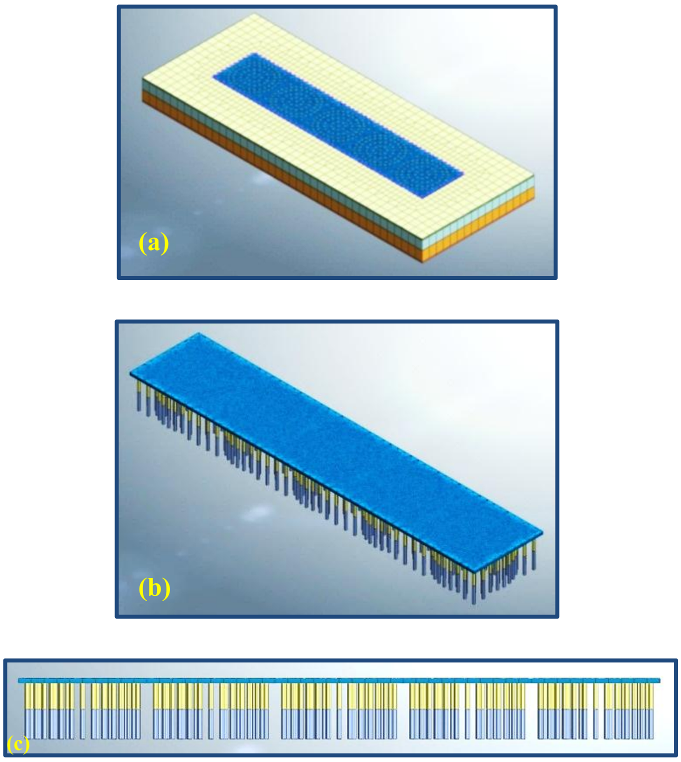

Fig. 8 Numerical model used in 3D Midas-GTS analysis, (a) total mesh (b) piled raft foundation (c) side view of piled raft foundation

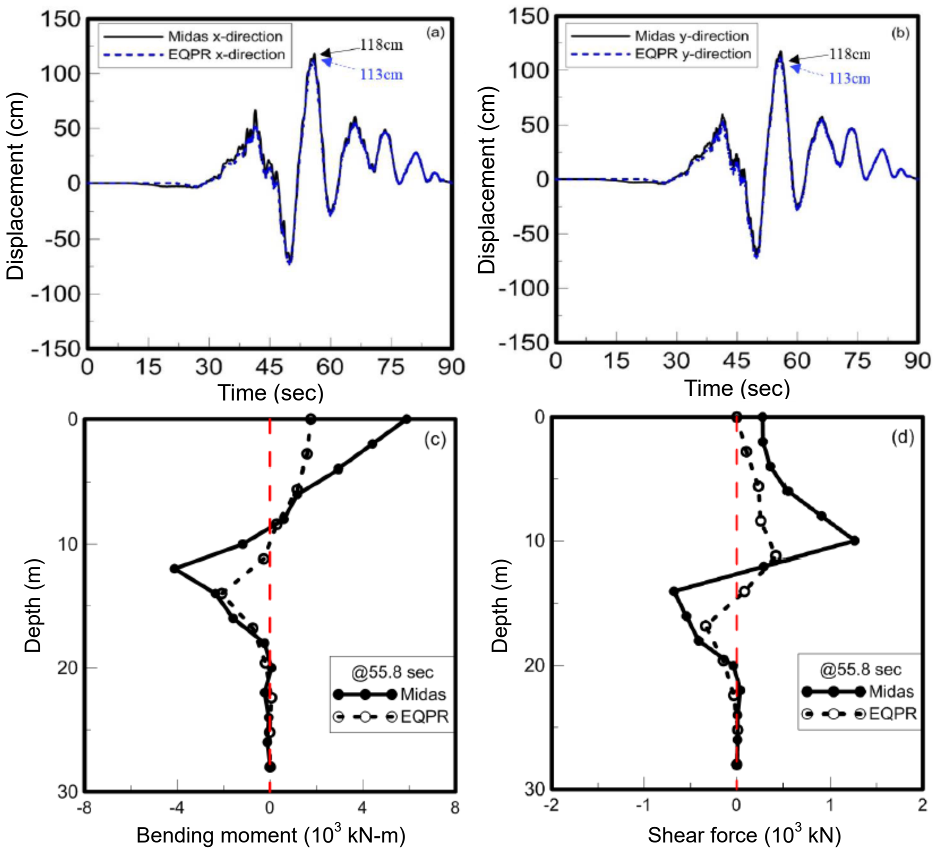

Fig. 9 Seismic responses of rectangular foundation on piles obtained from Midas and EQPR analysis: horizontal ground motions at (a) *x* direction and (b) *y* direction; internal stresses of (c) moment and (d) shear

Referring to the response of a single pile solution under the earthquake obtained earlier by Chang *et al.* (2016), it seems that the responses of piles and raft of the foundation will be governed by the ground motions. From the 3D FEM modelling, the pile responses were found dominated by the ground motions. Table 3 shows the required time for computations, the EQPR analysis seems to be a very efficient solution to the preliminary design. It will make the Performance Based Seismic Design (PBSD) much easier for the piled raft foundations.

4. STUDIES ON INFLUENCE FACTORS

The numerical model is studied herein based on the simplified analysis EQPR varying a number of model parameters to learn their effects. The parameters will include the dimensions of the piles (diameter and length), number of the piles, stiffness of the soil, thickness of the ground, and direction of the seismic motion as well as the existence of the superstructure. The standard model conditions used in the studies are listed in Table 4. Notice that the mass and stiffness of the superstructures are encountered in following studies. It can be found that the maximum displacements of the foundation can be reduced once the superstructure loads are applied.

4.1 Structural Dimension and Orientation

Varying the diameter of pile at 1, 1.5 and 2 meters for the numerical model subjected to horizontal seismic motions in x direction (longitudinal direction of the slab), the results of foundation displacements are plotted in Figs. 10(a), 10(b), and 10(c). It can be found that in Fig. 10(b), the absolute foundation displacements will be decreased from 96.62, 92.09 to 81.61 cm when reducing the pile diameter. This is because less loads will be transmitted through the pile-soil-pile elements (or equivalent piers) when smaller pile diameter is resulted. Displacement of the equivalent pier will not be affected much varying the pile diameter. The differences (15.17 ~ 30.18 cm) between the maximum displacements of foundation and ground surface (111.79 cm) are shown in Fig. 10(c). Smaller pile diameter will yield larger relative displacements between the foundation and ground surface, in which the structure would be more vulnerable to resist the ground movements.

By changing the pile length at 28, 22, and 16 meters, the results are plotted in Figs. 11(a), 11(b), and 11(c). It is noted that the absolute foundation displacements will become 96.62, 99.15, and 101.63 cm as the piles were shorten, and the corresponding difference between the foundation displacements and the surface ground displacements will be 15.13, 12.60, and 10.12 cm. The foundation displacement will be increased by reducing pile length. Notice that the embedded depth of the piles in the gravel is reduced from 15, 9 to 3 m (the thickness of soft soils remains the same). As the pile length decreases, the overall shear spring constant calculated will be enlarged, thus higher seismic forces transmitted will cause larger foundation displacement. However owing to the limited ground motions, the relative displacements between the foundation and ground surface are decreased. This can be interpreted by resistances of the end-bearing piles. Longer embedded piles will make the foundation harder to push whereas the shorter embedded piles are easier to move accordingly with the ground motions. This phenomenon needs special attention and it is limited to the presenting case.

Table 3 Computation time of the analyses on validated numerical model

Method	Computer features	Computation time (sec)
EQPR analysis	CPU: Intel Xeon E3-1231v3 RAM: 16GB	60 sec based on time increments of 0.0005sec (computations required for EQWEAP analysis is included)
3D Midas-GTS analysis		9hr 25min 10sec for 174780 elements based on time increments of 0.02 sec

Table 4 Parameters used in standard numerical model

Parameters	value	Units
Pile diameter	2	m
Pile length	28	m
Number of piles	93	per 60 m × 60 m area
Thickness of soft soils	13	m
Vs of soft soil	180	m/sec
θ	0	degree
R	0.5	N/A
m_{st}	1.5×10^8	kg

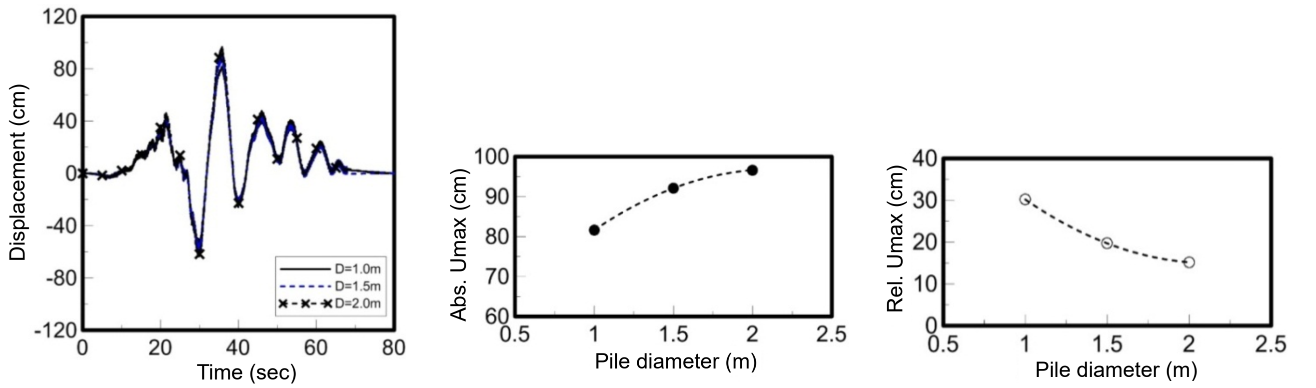

(a) Displacement time history (b) Maximum foundation displacements (c) Differences of maximum displacements between foundation and ground surface

Fig. 10 Effects of pile diameter on horizontal seismic response of rectangular foundation on piles

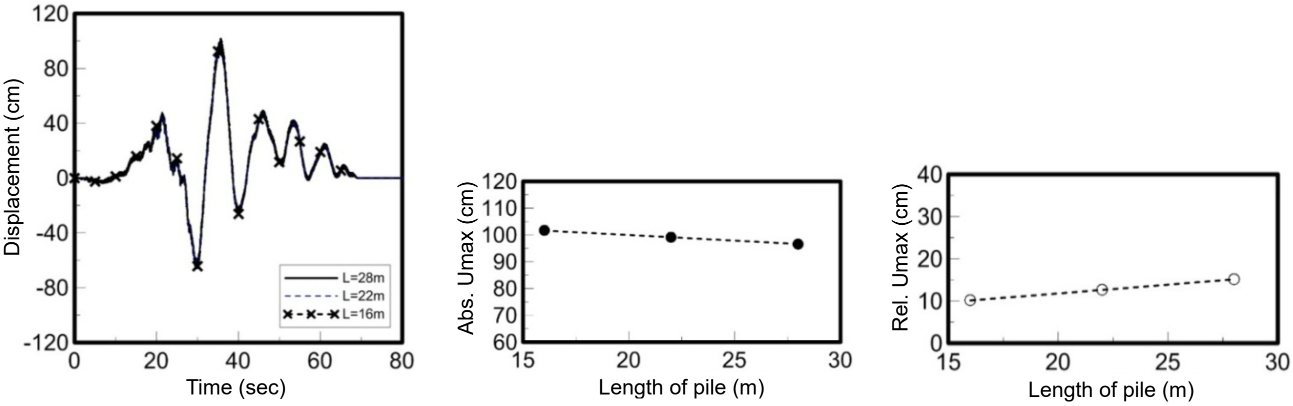

(a) Displacement time history (b) Maximum foundation displacements (c) Differences of maximum displacements between foundation and ground surface

Fig. 11 Effects of pile length on horizontal seismic response of rectangular foundation on piles

Reducing the number of piles in this case will barely change the foundation displacements. Figures 12(a), 12(b), and 12(c) reveal the results obtained by reducing the number of piles under each superstructure. Since the piles are oriented radially in rings from the center, the analysis is done by taking out the 2nd inner ring and the 3rd inner ring of piles, respectively, which will reduce the number of piles from 93, 77 to 69 under each superstructure. The absolute foundation displacements shown in Fig. 12(b) are 96.62, 95.44, and 93.70 cm as the number of piles was reduced. The relative displacements are about 15.13 ~ 18.05 cm. Reducing the number of piles by 17% and 26% in this case seems not affect the results significantly. The interferences between the amount of piles and the soils seem complicated to yield this observation. Again, one needs to very careful about the interpretation since the piles are seating on the firm layer.

4.2 Soil and Ground Conditions

The effects of the soft soils are studied varying the shear wave velocity of the soft soil at 120, 150, and 180 m/sec. The results are shown in Figs. 13(a), 13(b), and 13(c). It is interesting to see that the stiffer site will barely reduce the foundation displacement (97.26, 97.61, and 96.62 cm), the relative displacements are about 15.92, 15.16, and 15.13 cm. It is important to know that the observation is limited to this case of the end-bearing piles. To learn the possible effect of the thickness of soft soil, the thickness of soft layer is varied at 13, 18, and 23 meters (the corresponding embedded lengths of the piles in the gravel layer are 15, 10, and 5 meters). The results are shown in Figs. 14(a), 14(b), and 14(c).

In Fig. 14, the foundation displacement tends to decrease from 96.62, 96.06 to 93.25 cm with the increase of thickness of soft soil (the embedded length of pile drops from 15 m to 5 m), and the relative displacements are about 15.13, 17.27, and 18.25 cm. The differences are again insignificant compared to those found by reducing the diameter and length of piles. If the pile length remains, the effects of reducing the embedded pile length by increasing thickness of the soils seems to be trivial. It must be pointed out that the results are closely related to the spring constants calculated for the pile-soil-pile elements. The calculations involve not only the pile characters but also the material properties and thickness of the soil layers. The factors of shear wave velocity and thickness of the soft layer seem relatively unimportant in the case when end-bearing piles were encountered.

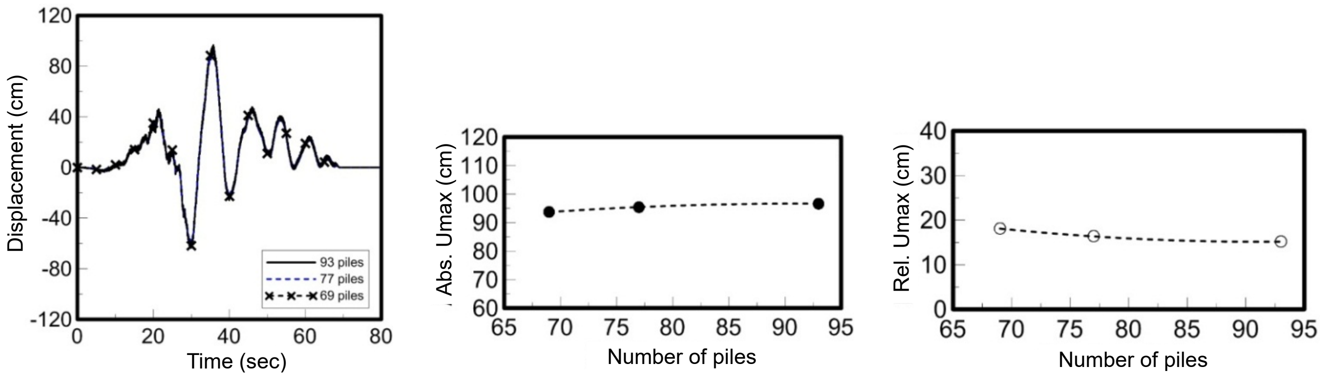

(a) Displacement time history (b) Maximum foundation displacements (c) Differences of maximum displacements between foundation and ground surface

Fig. 12 Effects of number of piles on horizontal seismic response of rectangular foundation on piles

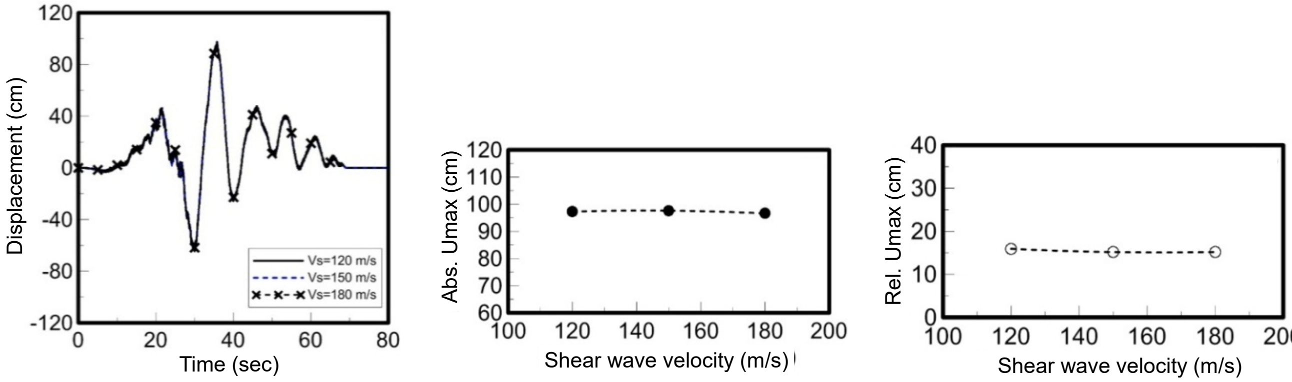

(a) Displacement time history (b) Maximum foundation displacements (c) Differences of maximum displacements between foundation and ground surface

Fig. 13 Effects of shear wave velocity of soft soils on horizontal seismic response of rectangular foundation on piles

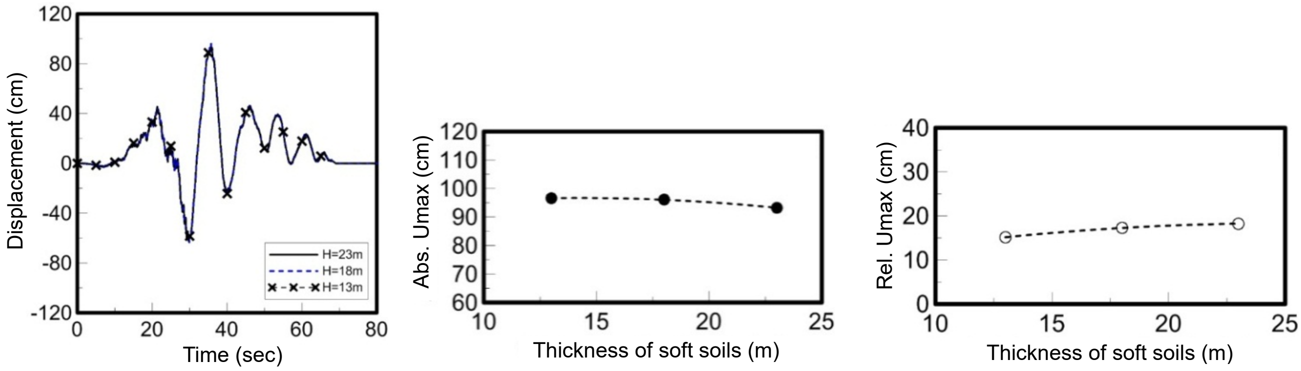

(a) Displacement time history (b) Maximum foundation displacements (c) Differences of maximum displacements between foundation and ground surface

Fig. 14 Effects of the thickness of soft soils on horizontal seismic response of rectangular foundation on piles

In contrast to show the effects of soft soil for foundation on floating piles, the results varying the shear wave velocity of soft soils at 120 ~ 180 m/sec with the thickness of 30 meters are plotted in Fig. 15. It can be seen from Figs. 15(b) and 15(c) that the foundation displacements are now affected more clearly by the shear wave velocity of soils. The foundation displacements become 94.07, 93.54, and 91.87 cm whereas the relative displacements between the foundation and ground surface are 20.75, 20.45, and 19.62 cm. Notice that the maximum ground displacements are 114.82, 113.99, and 111.49 cm in this case. It seems that as long as the piles are floating in the soils with constant thickness, a moderate changing of the soil stiffness will affect slightly the response of the rectangular foundation. Displacement differences between the foundation and the ground were found larger than those shown in the end-bearing piles.

Figure 16 shows the effects of thickness of soft soils on floating piles, those obtained by changing the thickness of soft layer at 30, 40, and 50 m are plotted in Fig. 16. The maximum

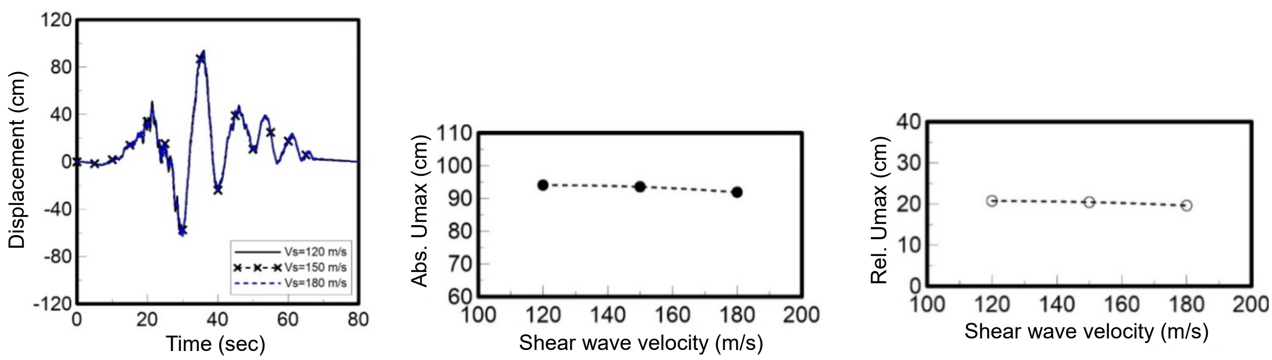

(a) Displacement time history (b) Maximum foundation displacements (c) Differences of maximum displacements between foundation and ground surface

Fig. 15 Effects of shear wave velocity of soft soils on horizontal seismic response of rectangular foundation on floating piles

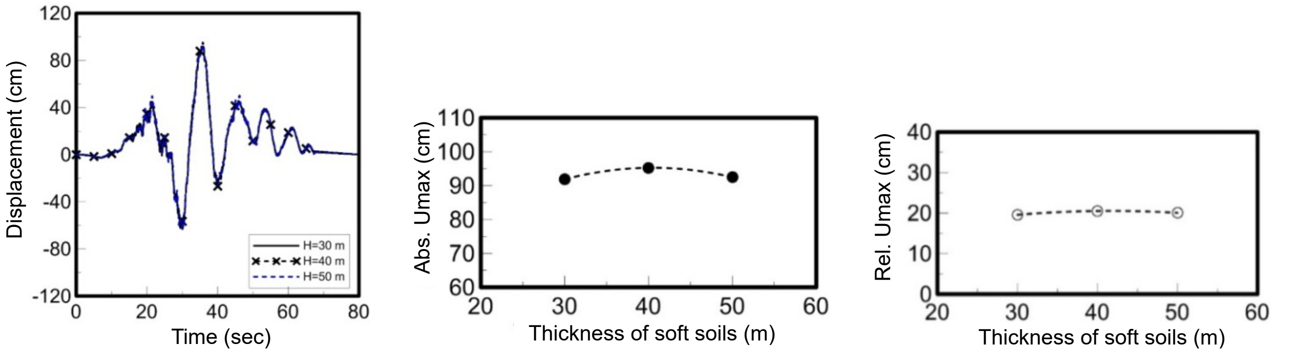

(a) Displacement time history (b) Maximum foundation displacements (c) Differences of maximum displacements between foundation and ground surface

Fig. 16 Effects of the thickness of soft soils on horizontal seismic response of rectangular foundation on floating piles

foundation displacements are now 91.87, 95.25, and 92.46 cm, and the relative displacements become 19.58, 20.53, and 20.06 cm. Notice that the maximum ground displacements are changing from 111.45, 115.78 to 112.52 cm. The relative displacements between the foundation and the ground surface were found larger in floating piles rather than those found in end-bearing piles.

Stiffness of the equivalent piers in above parametric studies are summarized in Table 5. It can be seen that the foundation displacements are highly correlated to the stiffness of the pile-soil-pile elements in the EQPR analysis.

4.3 Direction of Ground Motions

In order to learn the effects of the direction of ground motions with respect to foundation, bevel angles at 0° ~ 90° with the increments of 15 degrees are assigned for the same acceleration record. As it was shown in Figs. 17(a), 17(b), and 17(c), the foundation displacements seem not affected very much by the bevel angles. The maximum value of the absolute foundation displacements are noted as 96.62, 96.58, 96.57, 96.51, 96.34, 96.26, and 95.94 cm, whereas the corresponding relative displacements are 15.13, 15.17, 15.18, 15.24, 15.41, 15.49, and 15.81 cm. The foundation displacement in the x direction (longitudinal direction) becomes slightly larger than that found in the y direction (transverse direction) when the structure loads were applied. Relative displacements are gradually increased as the ground motion turned its direction from x- to y-axis. In comparison with the observations shown in Fig. 9, foundation displacements are reduced significantly due to the superstructure loads. Again, this observation is limited to the presenting model. It should be noted that the shape of the piled raft foundation, the embedded depth of the raft, and the geographic as well as the geological site conditions may influence the individual predictions.

Table 5 Stiffness of equivalent pier used in parametric studies

Section	Influence factor	Values			Stiffness of equivalent pier (GN/m)		
4-1	Pile diameter (m)	1.0	1.5	2.0	62.894	100.482	153.106
4-1	Pile length (m)	16	22	28	239.118	187.240	153.106
4-1	Number of piles	57	65	81	117.467	129.346	153.106
4-2	Shear wave velocity (m/sec) of soil soils-end bearing piles	120	150	180	152.115	152.561	153.106
4-2	Thickness of soft soils (m) - end bearing piles	13	18	23	153.106	144.661	136.216
4-2	Shear wave velocity of soft soils (m/sec) - floating piles	120	150	180	125.637	126.598	127.772
4-2	Thickness of soft soils (m) - floating piles	30	40	50	127.772	126.619	126.081

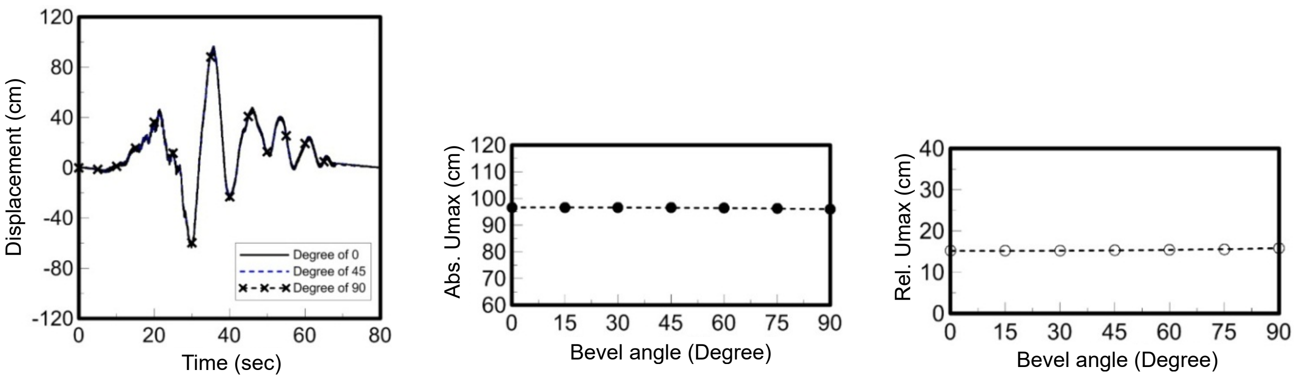

(a) Displacement time history (b) Maximum foundation displacements (c) Differences of maximum displacements between foundation and ground surface

Fig. 17 Effects of the bevel angle of ground motion on horizontal seismic response of rectangular foundation on piles

4.4 Influences of Superstructure Loads

As it was mentioned in section 2.2, the displacement ratio *R* is studied herein. By varying *R* at 0.1, 0.3, 0.5, 0.7, and 0.9, the corresponding effects on foundation displacements are shown in Figs. 18(a), 18(b), and 18(c). As one can tell, the superstructure motion could affect the foundation displacement significantly. For relatively rigid superstructure where the displacement ratio should be in a range of 0.1 ~ 0.9, the maximum foundation displacements were computed as 86.24, 90.67, 96.62, 102.83, and 108.96 cm whereas the relative displacements were found as 25.51, 21.08, 15.13, 8.92 and 2.79 cm. This observation indicates that the displacement of the superstructure will significantly affect the foundation responses and it should be monitored carefully as the time-dependent function.

To reveal the values of displacement factor *R*, the superstructure was taken as a single degree of freedom (SDOF) system mounting on the raft. The resolved foundation time-dependent accelerations can be treated as the base motions to solve for the associated motions of the superstructure. Time histories of the relative displacements and the absolute displacements as well as the time-dependent ratio *R* of the displacements can be shown in Figs. 19(a), 19(b), and 19(c). The displacement ratio *R* was found oscillating with time, its values are mainly varying in between 0.5 ~ 1.2. It can be seen that negative values of *R* do exist in this case. The calculations of *R* will have singularity problem, the analyst must be aware of it.

Figures 20(a), 20(b), and 20(c) depicting the influences of structural mass were conducted by varying *m* at 10% and 50% of its original value (150000 tons) with a fixed *R* at 0.5. It can be seen that the foundation displacement gradually increases from 96.07, 95.47 to 96.62 cm by reducing the mass of the structure. The corresponding relative displacements are 15.72, 16.32, and 15.17 cm. The mass of the superstructure was found less important to affect the foundation responses assuming that the displacement ratio *R* is fixed at 0.5. In reality, inertia effect of the superstructure would be combined with the effects of the superstructure impedance to affect the dynamics of the structure. The effects of the displacement ratio are affected by the inertia force as well.

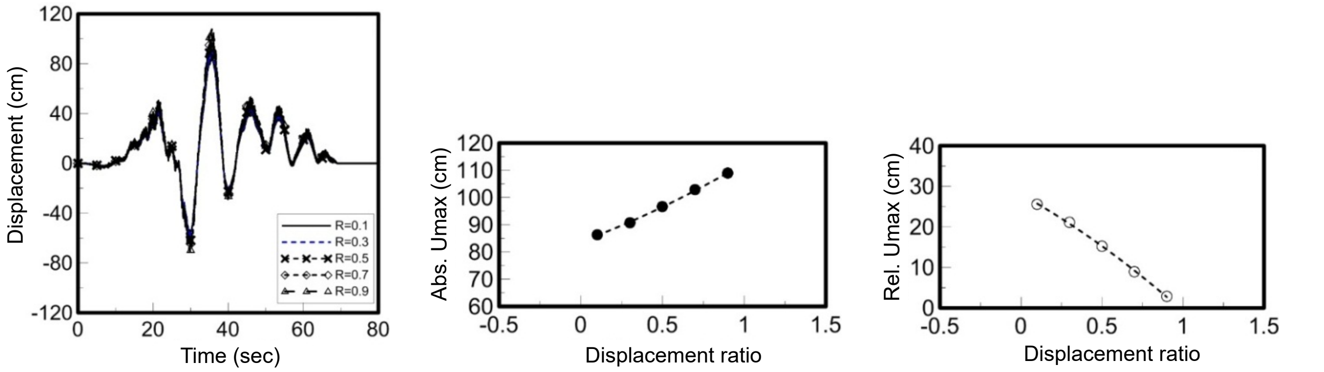

(a) Displacement time history (b) Maximum foundation displacements (c) Differences of maximum displacements between foundation and ground surface

Fig. 18 Effects of the motion of superstructure on horizontal seismic response of rectangular foundation on piles

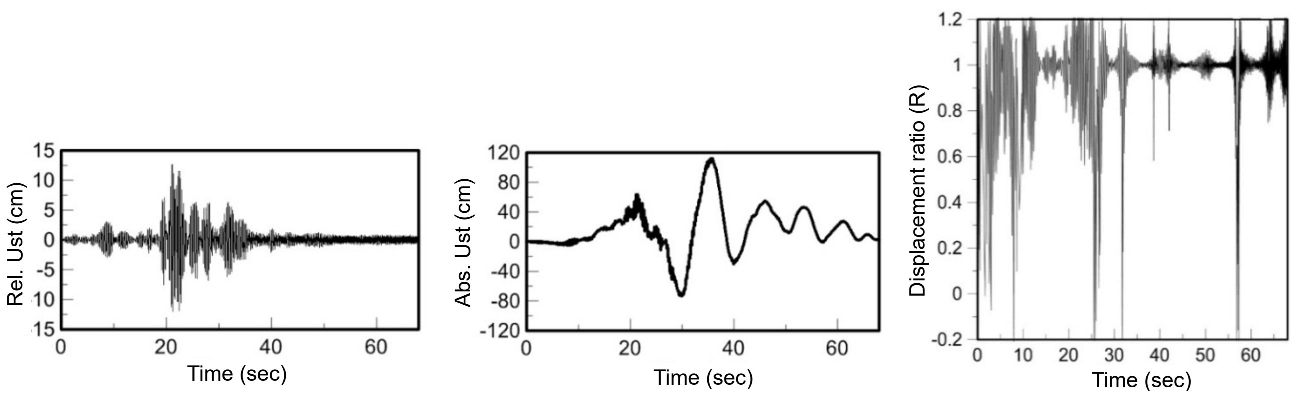

(a) Relative displacement time history (b) Absolute displacements time history (c) Displacement ratio *R* calculated as a time-dependent function

Fig. 19 SDOF motions of the superstructure subjected to the foundation shaking

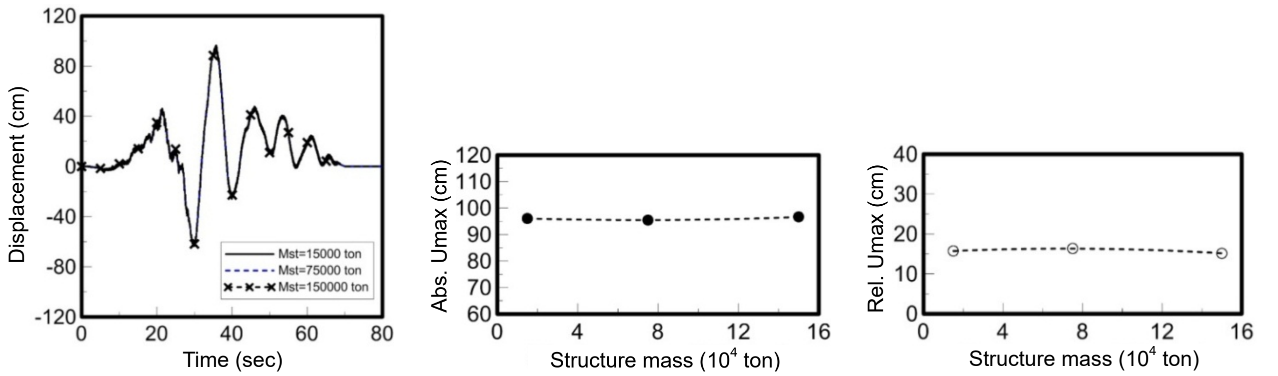

(a) Displacement time history (b) Maximum foundation displacements (c) Differences of maximum displacements between foundation and ground surface

Fig. 20 Effects of the mass of superstructure on horizontal seismic response of rectangular foundation on piles

5. CONCLUDING REMARKS

A simplified analysis called EQPR is suggested to monitor the seismic responses of a rectangular foundation on piles subjected to horizontal earthquake motions. Finite difference formulas were used to discretize the governing differential equation of the rectangular foundation whereas pile-soil-pile elements underneath the slab, the soils, and the superstructures upon the rectangular foundation were simulated properly using adequate shear springs. The simplified analysis is validated with 3D finite element analysis based on Midas-GTS program. Numerical model is given for rectangular foundation on piles at a site with relatively shallow soft soils underlain with gravels. The piles are seating in the layer of gravels. Parametric studies were able to conduct using such analysis. The conclusions of this study can be summarized as follows.

1. The simplified analysis can provide rational solutions to the seismic responses of rectangular foundation on piles in a very efficient manner. The computation time of such analysis is much less than that of a rigorous 3D finite element analysis. Therefore it could be conveniently used for PBSD of such foundation.
2. Based on the presenting numerical model, it is found that smaller pile diameter will reduce the foundation displacement. However larger relative displacements between the foundation and ground will be resulted. On the other hand, reducing the pile length (or embedded length of the piles) will slightly enlarge the foundation displacement; relative displacements between foundation and ground surface are decreased. The effect of changing the number of piles was found unimportant compared to the pile diameter and pile length.
3. The stiffness of the soft soil in terms of varying shear wave velocity of the soil in a range of 120 ~ 180 m/sec will not affect much of the foundation displacement when encountering the end-bearing piles. Trivial influences were found by varying the layer thickness of soft soils. Nevertheless, stiffer and thicker soft soils will help to reduce the foundation displacement. For rectangular foundation on floating piles, the influences of stiffness and thickness of the soils became more significant. The thickness of the soil layer should be monitored carefully since the foundation and ground may be amplified under the resonance. In general, foundation on end-bearing piles would cause smaller relative displacements than those obtained from floating piles.
4. The direction of the horizontal ground motion in association with the foundation seems to be an insignificant issue in such problem. The foundation displacement found by longitudinal ground excitation is slightly larger than that occurred by ground motions along the transverse direction of foundation. The analysts should be cautious knowing that the wave scattering effects of the piled raft foundation will occur when foundation is embedded in the soils.
5. The effect of superstructure is significant to the foundation displacement. The existence of the superstructure will generally reduce the foundation displacement. The more rigid the superstructure is (displacement ratio R becomes smaller), the less the foundation displacement will be. In reality, the displacement ratio R between the superstructure and the foundation is a time dependent value, and it can be mainly in a range of 0.5 ~ 1.2. By fixing the displacement ratio, the mass of the superstructure was found relatively unimportant. The importance of the dynamic effects of the superstructure should be monitored carefully.
6. Since the ground forces were mainly transmitting through the pile-soil-pile elements. The observations have limitations based on the usage of shear springs. Seismic design of the piled raft foundation needs to check the internal stresses of the piles too. The foundation displacements presented in this study are used only for explicit comparisons.

ACKNOWLEDGEMENTS

This paper is partial results of the research study supported by Ministry of Science and Technology (formerly National Science Council, NSC) in Taiwan through research grant NSC-102-2221-E-032-024-MY3. The authors would like to express their sincere gratitude for the support.

REFERENCES

Abderlrazaq, A., Badelow, F., Sung, H.K., and Poulos, H.G. (2011). "Foundation design of the 151 story Incheon Tower in a reclamation area." *Geotechnical Engineering*, **42**(2), 85–93.

Chang, D.W., Cheng, S.H., and Wang, Y.L. (2014). "One-dimensional wave equation analyses for pile responses subjected to seismic horizontal ground motions." *Soils and Foundations*, **54**(3), 313–328.

Chang, D.W., Lin, B.S., and Cheng, S.H. (2009). "Lateral load distributions on grouped piles from dynamic pile-to-pile interactions factors." *International Journal for Numerical and Analytical Methods in Geomechanics*, **33**(2), 173–191.

Chang, D.W., Lu, C.W., Lin, S.S., and Lai, J.R. (2016). "Dynamic analyses for seismic performance based design of geotechnical structures with examples in deep foundations." *Geotechnical Engineering*, **47**(2), 83–88.

Clancy, P. and Randolph, M.F. (1993). "Simple design tests for piled raft foundations." *Geotechnique*, **36**(2), 169–203

Gazetas, G. (1991). "Foundation vibrations." Chapter 15, *Foundation Engineering Handbook*, ed. Fang, H.Y., Springer, 553–593.

Hong, M.Y. (2016). "Case studies on static and dynamic behaviors of piled raft foundations." Master Thesis, Department of Civil Engineering, Tamkang University, Tamsui, New Taipei City, Taiwan.

Horikoshi, K. and Randolph, M.F. (1996). "Estimation of overall settlement of piled rafts." *Soils and Foundations*, **39**(2), 59–68.

Katzenbach, R. (1993). "The technical and economic importance of the combined piled raft foundation represented by examples of high rise buildings." *Bautechniks*, **70**(3), 161–170.

Katzenbach, R. and Choudhury, D. (2013). *ISSMGE Combined Pile-raft Foundation Guideline*, Technische Universitat Darmstadt, Institute and Laboratory of Geotechnics, Darmstadt, Germany.

Katzenbach, R., Choudhury, D., and Chang, D.W. (2013). "General report of TC212 deep foundations." *Proc., 18th ICSMGE*, Paris, France, 2651–2658.

Kitiyodom, P. and Matsumoto, T. (2002). "A simplified analysis method for piled raft and pile group foundations with batter piles." *International Journal for Numerical and Analytical Methods in Geomechanics*, **26**, 1349–1369.

Kitiyodom, P. and Matsumoto, T. (2003). "A simplified analysis method for piled raft in non-homogeneous soils." *International Journal for Numerical and Analytical Methods in Geomechanics*, **27**, 85–109.

Kitiyodom, P., Matsumoto, T., and Kawaguchi, K. (2005). "A simplified analysis method for piled raft foundations subjected to ground movements induced by tunneling." *International Journal for Numerical and Analytical Methods in Geomechanics*, **29**, 1485–1507.

Kobayashi, H., Nishio, H., Nagao, T., Watanabe, T., Horikoshi, K., and Matsumoto, T. (2009). "Design and construction practices of piled raft foundations in Japan." *Proc., Int. Conf. on Deep Foundations-CPRF and Energy Piles*, 101–135.

Kouroussis, G., Anastasopoulos, I., Gazetas, G., and Verlinden, O. (2013). "Three-dimensional finite element modeling of dynamic pile-soil-pile interaction in time domain." *Proc., 4th ECCOMAS Thematic Conference on Computational Methods in Structural Dynamics and Earthquake Engineering*, Kos Island, Greece.

Matsumoto, T. (2013). Personal communications-lecture notes on piled raft foundations.

Midas GTS (2012). *User Manual*, MIDAS Co.

Poulos, H.G. (1991). "Analysis of piled raft foundations." *Computer Methods and Advances in Geotechniques*, ed. Beer *et al.*, Balkema, Rotterdam, 153–191.

Poulos, H.G. (2001). "Pile-raft foundation: Design and applications." *Geotechnique*, **51**(2), 95–113.

Randoplh, M.F. and Clancy, P. (1993). "Efficient design of piled rafts." *Proc., Deep Foundations on Bored and Auger Piles*, Ghent, 119–130.

Randolph, M.F. (1994). "Design methods for pile groups and piled rafts." *Proc., 13th ICSMGE*, New Delhi, Rotterdam, Balkema, **5**, 61–82.

Yamashita, K., Kakurai, M., and Yamada, T. (1994). "Investigation of a piled raft foundation on stiff clay." *Proc., 13th ICSMGE*, New Delhi, Rotterdam, Balkema, **3**, 543–546.

Yamashita, K., Tanikawa, T., and Hamada, J. (2015). "Applicability of simple method to piled raft analysis in comparison with field measurements." *Geotechnical Engineering*, **46**(2), 43–53.